Measurement of a Single-Slit Diffraction Pattern Using a Sliding Slit

Introduction

Diffraction is a wave phenomenon where, as a wave propagates through a small aperture, it spreads out [1]. One method to measure the diffraction pattern involves projecting it onto a screen. Traditionally, this constitutes measuring the light intensity at each point in the pattern [2-3]. This may involve capturing a picture of the diffraction pattern and measuring the light intensity at each discrete point via image analysis software [3]. Fig. 1 below shows an example apparatus [3].

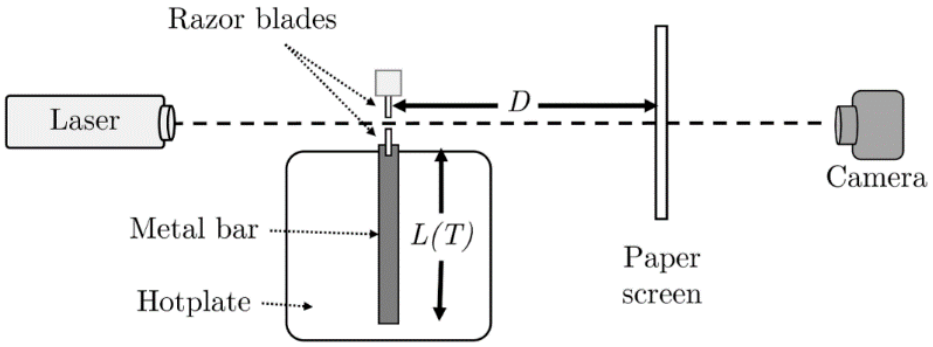

Figure 1: Example apparatus that measures the diffraction pattern of a variable single slit, where the slit width narrows as the heated metal bar expands.

Alternatively, researchers from the University of North Carolina at Charlotte demonstrated the local intensity of different points on the diffraction pattern also can be obtained by refracting the diffracted light beam with a piece of motorized glass [4]. This apparatus measures the intensity profile as a continuous entity [4]. Fig. 2 below shows their experimental setup [4].

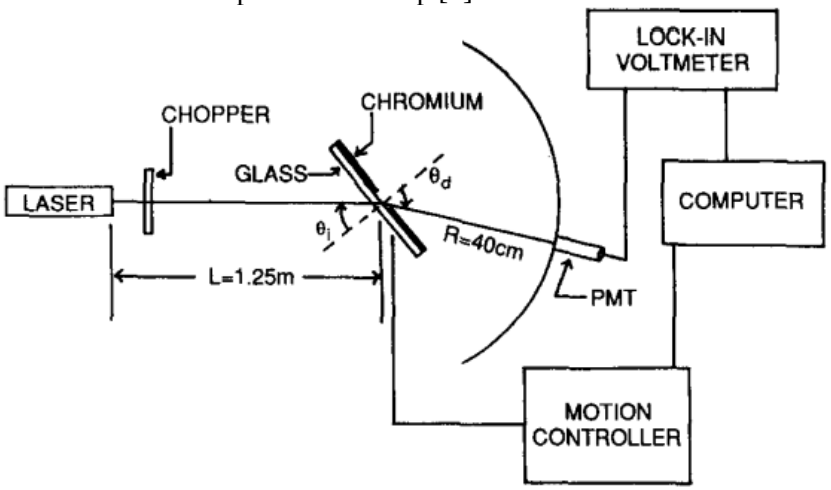

Figure 2: Example apparatus that measures a diffracted beam continuously by refracting it into the PMT, which acts as a light intensity sensor.

We propose an alternative method. If we slide a light intensity sensor along the diffraction pattern at a constant velocity and restrict it with another slit that is small compared to the diffraction pattern, we can measure the intensity profile as a continuous entity. We will refer to this concept as the "sliding slit apparatus". This investigation aims to answer the following research question: how effective is the "sliding slit apparatus" at measuring the one-dimensional intensity profile of a single-slit diffraction?

Theory

Suppose we have the experimental setup for single-slit diffraction shown in Fig. 3 below.

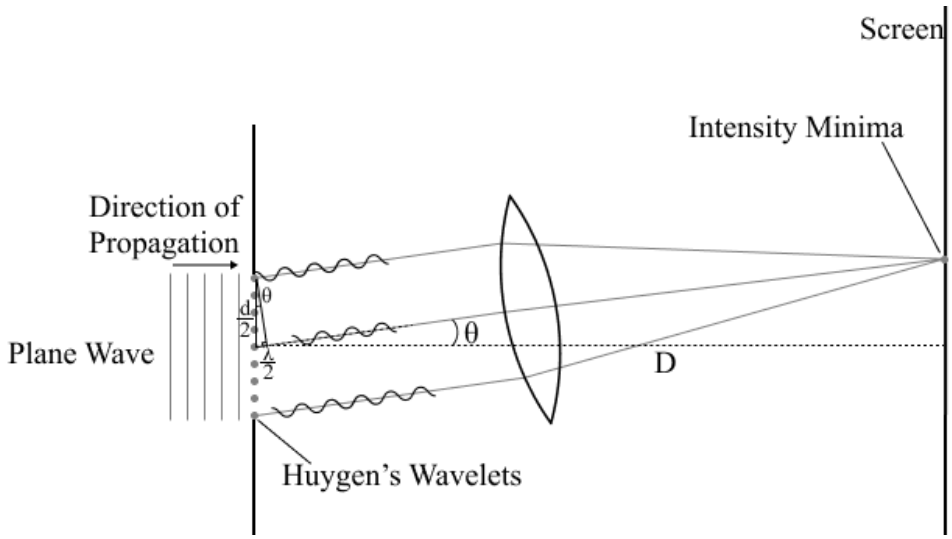

Figure 3: Geometry of the destructive interference present in single-slit diffraction.

A plane wave propagates towards the slit. As it goes through the slit, we can assume that at any arbitrary point, there will be a Huygen's wavelet and it emits a spherical wavefront that starts in phase with all other emitted wavefronts in between the slits. The gray points in Fig. 3 represent these wavelets. We can draw a line that connects a wavelet to a fixed location on the emitted wavefront and trace its path as it propagates over time. We chose these locations such that all the lines produced by different wavelets are parallel, then focused them onto a single point on the screen with a lens, as shown in Fig. 3 above. These lines represent the path traveled by each wavefront to arrive at a certain point on the screen.

As they propagate toward the screen, the waves interfere with each other. When multiple wavefronts are half a wavelength out of phase with each other, they destructively interfere and produce an intensity minimum point.

We assume the intensity profile strictly follows the Fraunhofer model, which assumes that *D*, the distance between the slit and the screen, is large enough such that the spherical wavefronts emitted by each of the Huygen's wavelets can be perceived as planar [5]. Using this assumption, the following equation shows the relationship between *s*, the location of the m^{th} intensity minimum, and both d, the slit width, and λ, the wavelength of the light:

$$s = \frac{m\lambda D}{d}$$

We know that the single-slit diffraction intensity pattern is related to the path difference between two wavefronts emitted by two different Huygen's wavelets. Their path difference determines the strength of their mutual interference, which determines the intensity at different points on the screen. The intensity pattern is characterized by a squared sinc function [6]:

$$I = I_0 \left(\frac{\sin\beta}{\beta}\right)^2$$

where I_0 is the maximum intensity. To find the relationship between θ and β, we must use the phasor method, a commonly used technique for analyzing sinusoids [6-7]. The following equation shows the phasor that represents the relative magnitude of intensity at an arbitrary angle:

$$I = e^{i\phi}$$

where ϕ represents the phase at a specified point, which in this case, is an angle that represents the path difference between any two wavefronts projected to an arbitrary point on the screen in Fig. 3. The following expression describes ϕ mathematically:

$$\phi = \left(\frac{2\pi}{\lambda}\right) d \sin\theta$$

In Fig. 4a below, we can also see that the red triangle and the small, black triangle, are similar triangles. Fig. 4b shows a zoomed-in view of the small, black triangle. The net effect of the destructive interference between the two wavefronts is equivalent to projecting a dimmer wavefront, whose path bisects the angle θ, onto the screen, as shown through the lighter red line.

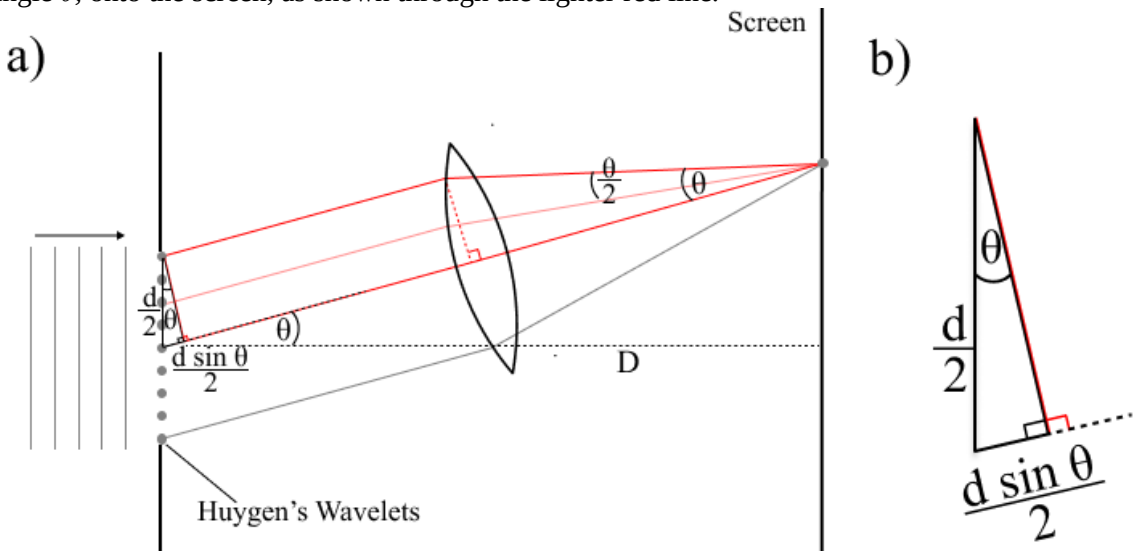

Figure 4: The geometrical relationships between the triangles formed by the wavefronts emitted by two different Huygen's wavelets.

Hence, the path length of the equivalent wavefront must equal the average path length of the two wavefronts that interfered with each other. Its path difference to either of the initial wavefronts represents β. Therefore, β must be [6]:

$$\beta = \frac{\phi}{2} = \frac{\pi d \sin\theta}{\lambda}$$

After substituting β into the squared sinc function, we produced Eq. 1 below, which determines the intensity profile of the diffraction pattern [6]:

$$I = I_0 \left(\frac{\lambda \sin\left(\frac{\pi d \sin\theta}{\lambda}\right)}{\pi d \sin\theta} \right)^2 \qquad (1)$$

We can also find the location on the screen where these wavefronts are projected to through the angle θ and the distance between the slit and the screen using the following equation:

$$s = D \tan\theta$$

We used Eq. 1 to calculate the theoretical intensity profile and compared it to the measured intensity profile.

Methodology

The "sliding slit" was constructed by mounting a Vernier light intensity sensor to a screen and the screen to a linear actuator. The sensor has an optimal operating range of 0-600 lux and any measurement higher than 750 lux caused saturation. It recorded 1000 measurements per second. Fig. 5 below shows the layout of the apparatus.

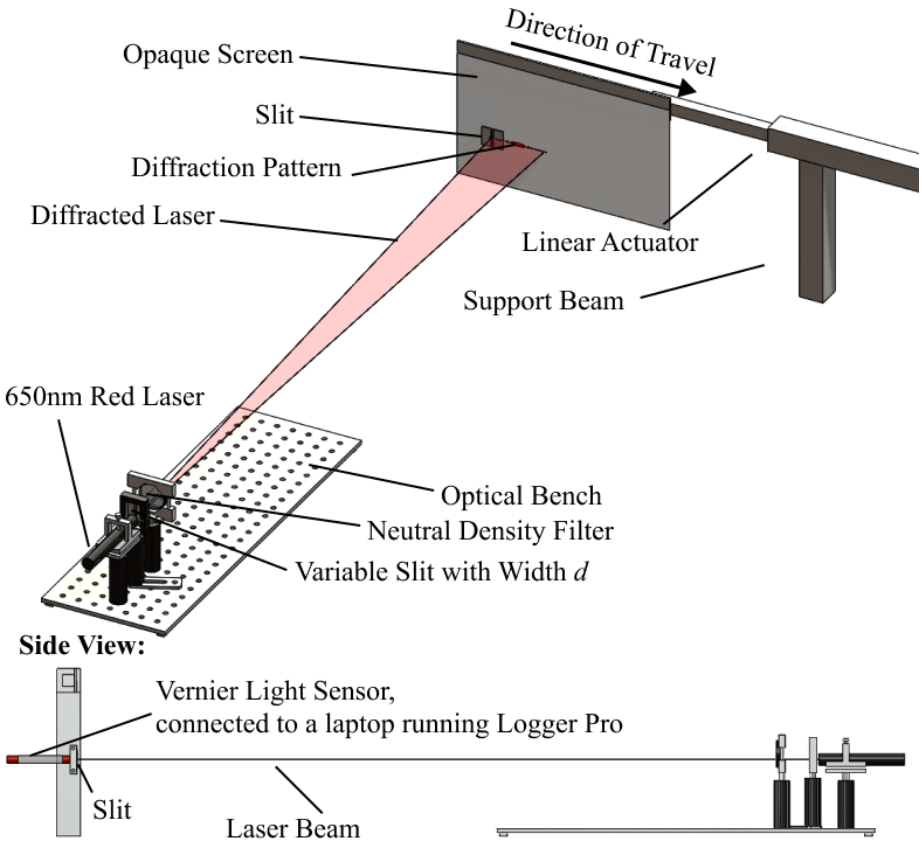

Figure 5: General layout of the apparatus.

A red laser, with a wavelength of 650nm ± 10nm, was aligned with a variable width slit, whose width is controlled by a micrometer, and a neutral density filter. The laser beam was diffracted by the slit, then projected onto the opaque screen. We added a neutral density filter to reduce the peak intensity of the diffracted beam, such that it falls in the operating range of the Vernier light intensity sensor.

The light sensor was mounted behind the opaque screen, with two razor blades taped to the screen to create a fixed width slit, restricting the sensor's field of view. We experimented with the slit width and varied it until the maximum intensity produced by the narrowest width of the variable slit measured at approximately 580 lux. We needed the maximum intensity to be as close to the maximum of the operating range as possible to ensure the darker fringes would be measured clearly. We also did not change the width of the fixed slit to ensure the magnitude of the effect of convolution was consistent. Convolution means when a function overlaps with another function, they "blend" together [9]. In this case, the measured intensity is the average intensity of all discrete points in the sensor's field of view. As the slit width increases, the more the function "blends". Since the fixed slit has a width of just 70μm, whereas the widths of the full, measured diffraction patterns are approximately 10cm, the width of the fixed slit is very narrow relative to the full diffraction patterns. Therefore, the effect of convolution on the intensity profile must be insignificant, and hence it is not factored into the theory.

The screen was mounted onto a linear actuator that slid from one side of the diffraction pattern to the other. The portion of the actuator that extended was attached to a threaded rod and a motor rotated a nut on the rod to convert the rotating motion into a linear motion at a constant velocity. The light intensity sensor was connected to a laptop running Logger Pro, a software that allows one to configure and command the sensor [8]. The sensor recorded the light intensity 1000 times per second. We measured the intensity profiles of eight different slit widths, with 10 trials for each. We also measured the velocity of the actuator by attaching a "picket fence" (see Fig. 6 below).

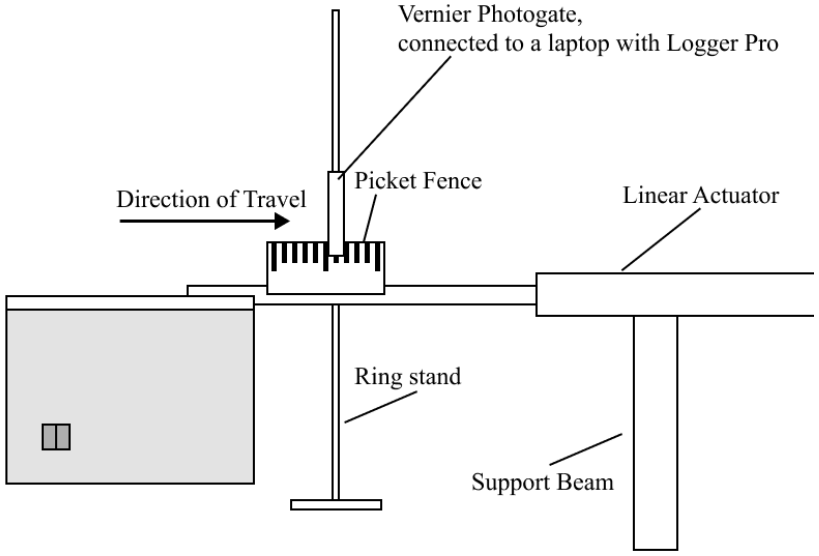

Figure 6: Apparatus for determining the velocity of the linear actuator.

The photogate was set in gate mode, and it recorded the elapsed time whenever it first encountered a picket on the picket fence.

Results and Analysis

Since the actuator was moving at a constant velocity, we can assume that the change in position of the slit is proportional to the elapsed time, and the slope of its linear best fit line would represent the actuator's velocity. Fig. 7 below shows a sample position-time plot used to determine the velocity of the actuator. Since the error bars are smaller than the data points on the graph, they are omitted.

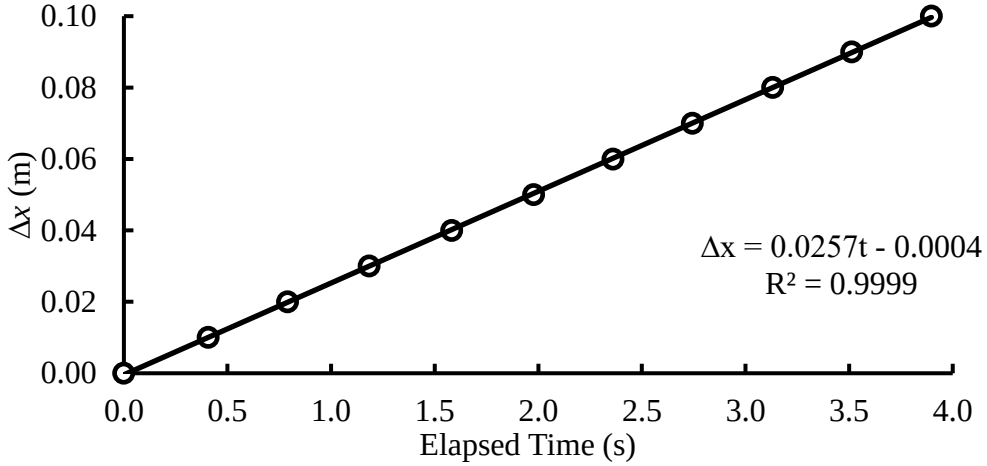

Figure 7: The position-time plot of trial 1.

We created a position-time plot for each of the 10 trials and averaged the slopes of their linear best fit line. Table 1 below shows the experimental velocity derived from each of the trials.

Table 1: The experimentally derived velocity of the actuator.

Trial #	**1**	**2**	**3**	**4**	**5**
Velocity (m/s)	0.0257	0.0261	0.0259	0.0254	0.0255
Trial #	**6**	**7**	**8**	**9**	**10**
Velocity (m/s)	0.0257	0.0252	0.0255	0.0252	0.0257
v_{avg}	0.0256 m/s				

The average velocity of the slide, 0.0256 m/s, has a very small random error, considering all values derived from different trials are within 0.0005 m/s of the average velocity. We accepted 0.0003 m/s, the standard deviation between different trials rounded to a single decimal place, as the random uncertainty of the velocity.

The narrowest slit width we used was 100μm ± 5μm, and the slit width is increased by 20μm per step, to a maximum slit width of 240μm. The slit widths were measured with a traveling digital microscope.

Since the maximum intensity is dependent on the maximum light flux allowed through the slits, as the width of the variable slit increases, the peak intensity increases. Hence, we placed neutral density filters with different optical densities (OD) to decrease the light intensity such that the maximum intensity recorded was in the range of 500 and 700 lux. This range is within the operating range of the sensor (0-750 lux) while ensured that the dimmer fringes could be detected. However, for both the 160μm and the 240μm slits, we were unable to obtain a measurement of the intensity profile within the operating range of the sensor. Fig. 8 below shows the measured intensity profile of the diffraction pattern of the 160μm slit.

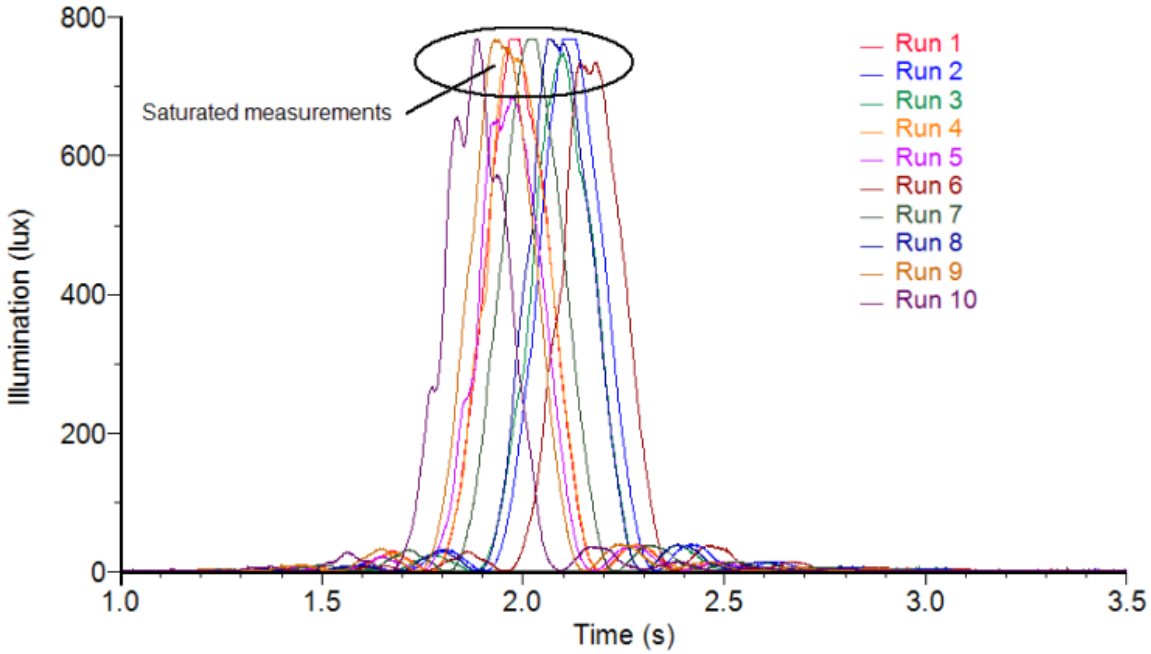

Figure 8: Intensity profile graph produced by a slit with a width of 160μm ± 5μm.

Many trials showed a flattening of the central lobe, which indicates that the light sensor was saturating. This indicates that the maximum intensity of the center lobe was beyond the maximum intensity that the sensor could accurately measure. Although narrowing the fixed slit would reduce the measured light intensity, we did not do so due to our concern about altering the magnitude of the effect of convolution on the diffraction pattern. We kept the slit width fixed to ensure both the effect of convolution and the random error stayed consistent. We then tried to reduce the maximum intensity by reducing the height of the slit, but this had no significant effect on the maximum intensity.

To reduce saturation, a neutral density filter was inserted in front of the lens. However, using the 0.6 OD neutral density filter, the sensor was still saturated. We also tried the 0.9 OD neutral density filter, but all fringes further away than the first intensity minima on each side of the center lobe became undetectable, suggesting the optimal OD lies somewhere between 0.6 and 0.9. However, these were the only available filters. Since we could not eliminate the saturation, we decided to abandon the measurements generated by the 160μm slit. We encountered a similar issue with the 240μm slit, where even with the 0.9 OD neutral density filter the sensor remained saturated. We tried to stack the two neutral density filters together, effectively creating a filter with an OD of 1.5, but this caused the dimmer fringes to become

indetectable. Therefore, we also abandoned the measurements generated by the 240μm slit. Nonetheless, we still had measurements from 6 different slit widths: 100μm, 120μm, 140μm, 180μm, 200μm, and 220μm.

We shifted each measured intensity profile to align them with our theoretical model. Fig. 9 below shows an example transformation of the intensity profiles.

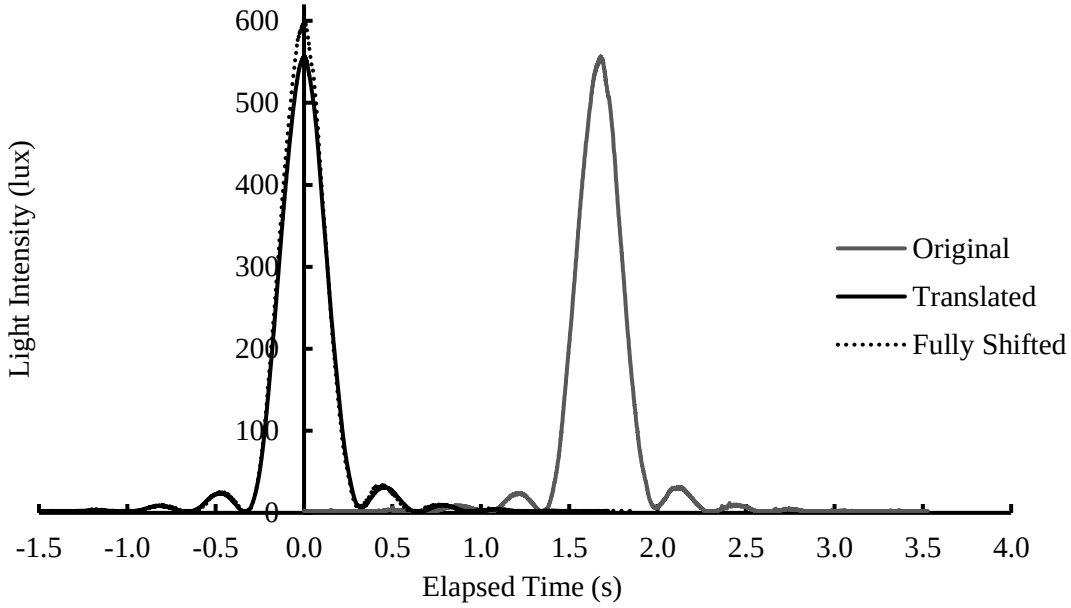

Figure 9: Intensity profile transformation for trial 1 of the 100μm slit.

We first horizontally shifted the pattern such that the point of maximum intensity corresponded to $x = 0$. We then vertically stretched the pattern so that the maximum intensity, $I_0 = 600$. Then, we averaged the intensity values across all ten trials. We deemed the intensity profiles "fully shifted" once we completed this series of transformations.

Then, we transformed the x-axis from elapsed time to distance from the center lobe, in units of meters, using the average velocity of the linear actuator. Since velocity represents the change in position over time, we can use the following expression to find the change in position:

$$\Delta x = v_{avg}\Delta \mathrm{t}$$

We found the angle θ for each point on the screen, in relation to their distance from the center lobe, using the following equation:

$$s = D\tan\theta$$

$$\theta = \tan^{-1}\left(\frac{s}{D}\right)$$

We then calculated the theoretical intensity pattern using Eq. 1:

$$I = I_0\left(\frac{\lambda \sin\left(\frac{\pi d \sin\theta}{\lambda}\right)}{\pi d \sin\theta}\right)^2 \qquad (1)$$

We only compared the measured and the theoretical intensity profiles between the third minima on either side of the center lobe, because all fringes further away from the center lobe did not appear in the measurements consistently. They were also fluctuating chaotically.

A path difference of $\frac{\pi}{2}$ occurs when $\frac{\pi d \sin\theta}{\lambda} = \pm n\pi$, where n is an odd integer. When a path difference of $\frac{\pi}{2}$ occurs, an intensity minimum occurs, as all the wavefronts have completely and destructively interfered with each other. Hence, the third minima on either side occur at $\frac{\pi d \sin\theta}{\lambda} = \pm 5\pi$. Consequently, we discarded all values generated by the equation when $\left|\frac{\pi d \sin\theta}{\lambda}\right| > 5\pi$. Fig. 10 below shows the comparison between the fully shifted and averaged intensity profiles of each slit width.

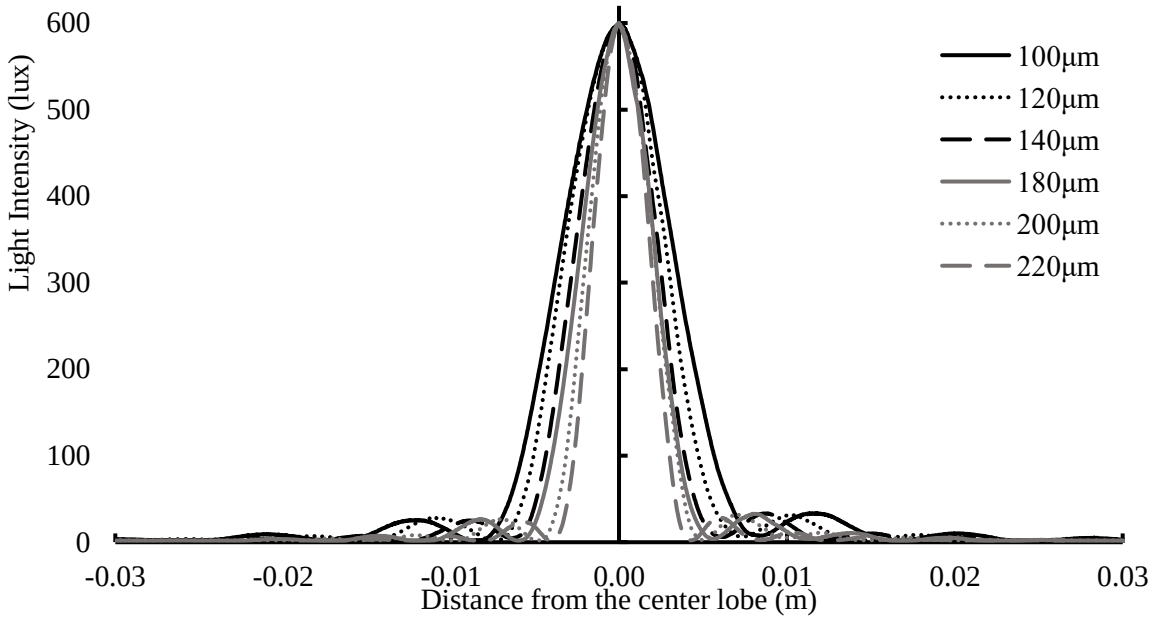

Figure 10: Comparison between the intensity profiles produced by various slit width.

We observe that the width of the center lobe decreases as the slit width increases. This is consistent with the basic theory behind single-slit diffraction. Also, since the theoretical intensity profile is an even function, the pattern should be symmetrical. However, the patterns shown in Fig. 10 are slightly asymmetrical. Fig. 11 below shows this asymmetry by comparing the location of the n^{th} intensity minima relative to the center lobe for the two different slit widths where this asymmetry is the most apparent.

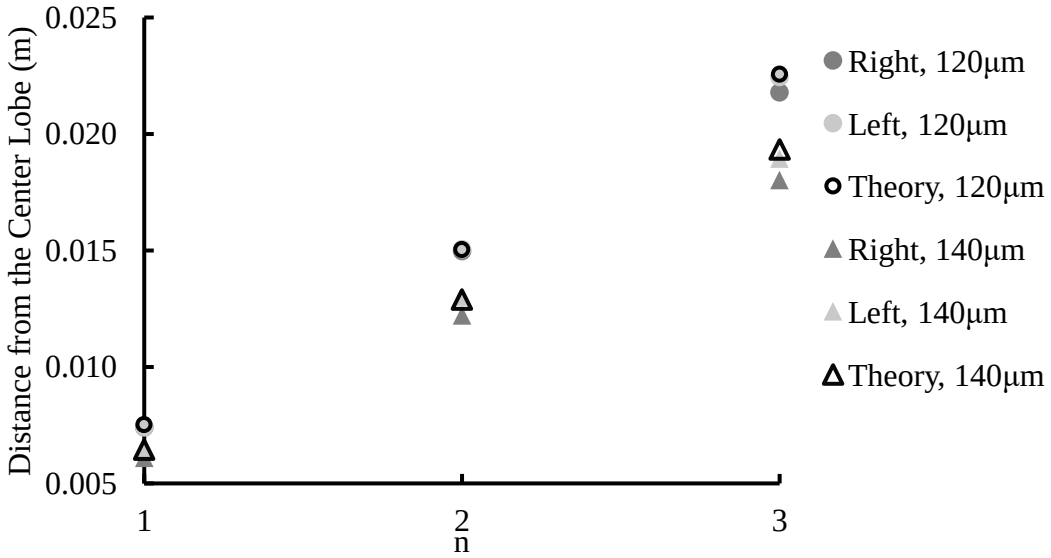

Figure 11: Comparison of the theoretical and the measured location of the intensity minima.

While the location of the intensity minima from the left is overlapping with the theory, the ones from the right are slightly displaced from the theoretical locations. We initially thought this was caused by the load on the linear actuator causing it to travel at a slight angle. Let us imagine the actuator as a lever, as shown in Fig. 12 below.

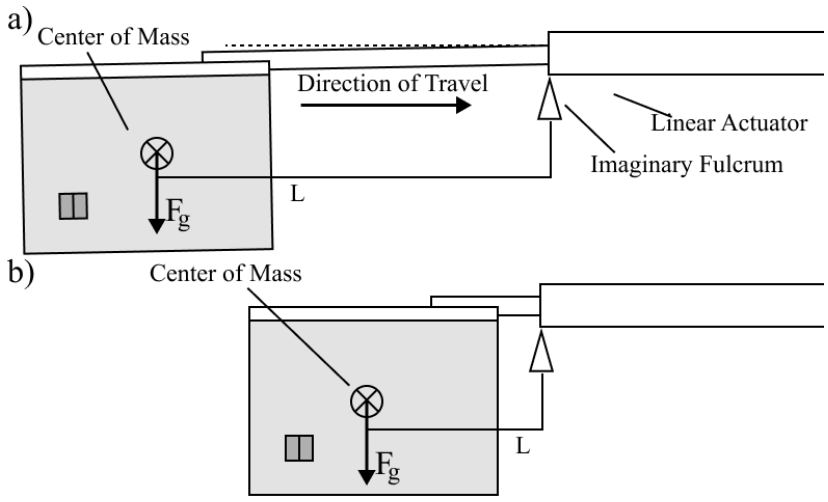

Figure 12: Rotational moment on the linear actuator, imposed by the load.

Since its moment is directly proportional to the distance between the center of mass of the load and the fulcrum, labeled as *L* in Fig. 12, when the linear actuator is fully extended, it experienced the greatest amount of moment, causing it to pitch down. This caused the light intensity sensor to measure a slightly rotated diffraction pattern. However, as the load retracted, the moment reduced, and the actuator returned to moving horizontally. This can partially explain why the right side of the diffraction pattern, measured when the actuator was further extended, does not fully match with the theory, whereas the left side, measured when it was mostly retracted, matches with the theory. However, since the linear actuator was only pitching down at a very small angle, its impact on the diffraction pattern should be quite minor. In comparison, the difference between the measured location of the minima on either side of the center lobe for the 140μm slit, relative to the theoretical location, is approximately 5.5%, which is quite significant. Therefore, even if the linear actuator pitching down has had an impact on the measurements, it cannot account for the 5.5% difference.

We also eliminated the possibility that this distortion is caused by the linear actuator not traveling at a constant velocity since the change in displacement of the actuator is directly proportional to the elapsed time (see Fig. 7 on page 7). The effect of convolution also cannot be the cause of this asymmetry, because its impact must be symmetrical since the theoretical intensity profile is an even function. Also, if the measured pattern is convoluted, it should be wider than the theoretical intensity profile. However, for all slit widths, except the 180μm slit, the measured profile is narrower than the theory, as shown in Fig. 13 below. This further suggests that the effect of convolution did not cause asymmetry in measurements.

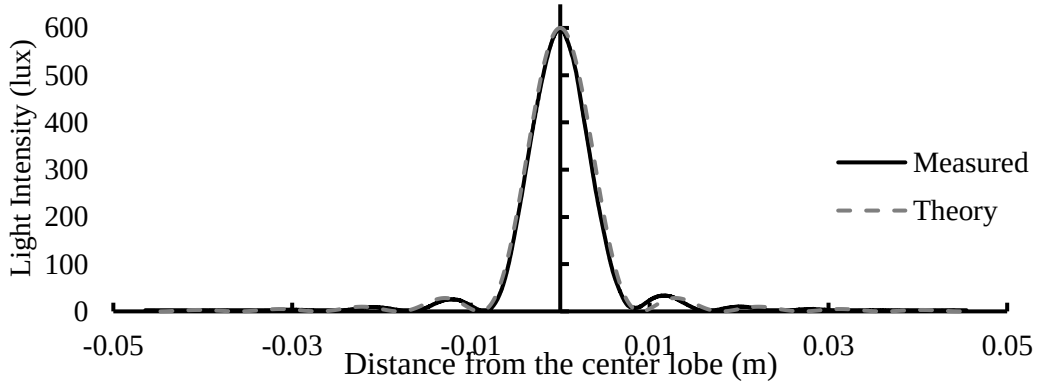

Figure 13: Theoretical and measured intensity profile produced by a 100μm slit.

Fig. 13 represents the typical case for all the measurements, whereas Fig. 14 below shows the outlier case, where the measured intensity profile is wider than the theory.

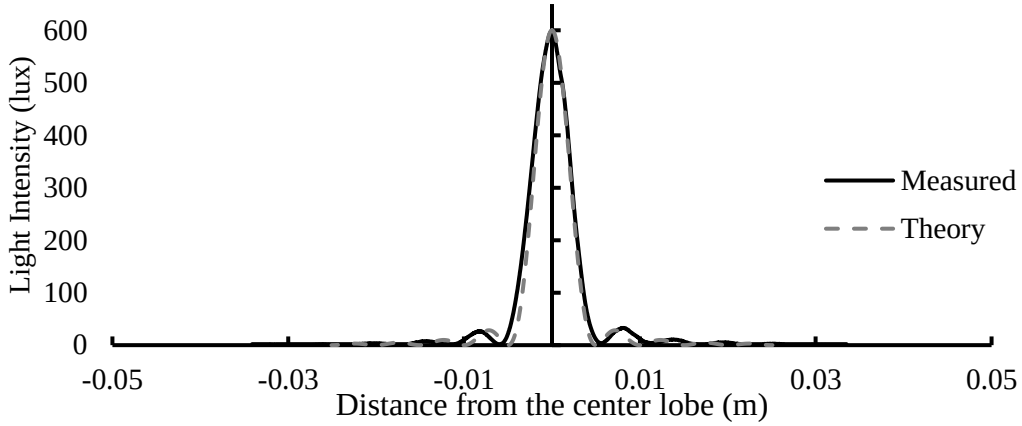

Figure 14: Theoretical and measured intensity profiles produced by a 180μm slit.

A possible cause for the measured intensity profiles to be narrower than the theory is that the linear actuator's velocity is affected by its battery level. We used the same motor and battery for a different application and noticed that the motor spun marginally faster when the battery is fully charged, by approximately 2%. If the actuator operated at a higher velocity when it measured the diffraction pattern, the real diffraction pattern could be marginally wider than the measured. Therefore, battery level may have had an impact on the measured intensity profiles. Nonetheless, its impact is likely to be quite minor because we recorded the battery level for every trial and the entire experiment only depleted less than 10% of the battery's total charge.

Since for most slit widths, the measured profile is narrower than the theory, this indicates the effect of convolution likely only had a minor impact on the measured patterns. Since we were still unsure of the cause of the asymmetry in the measurements, we then doubted if it was caused by our method of manually aligning the measured and the theoretical pattern. We tested this idea by translating the measured intensity profiles such that the distance between the center of the pattern and the first intensity minima on the left is the same as the first minima on the right. Fig. 15 below shows the comparison between the theoretical profile and the horizontally translated measured profile.

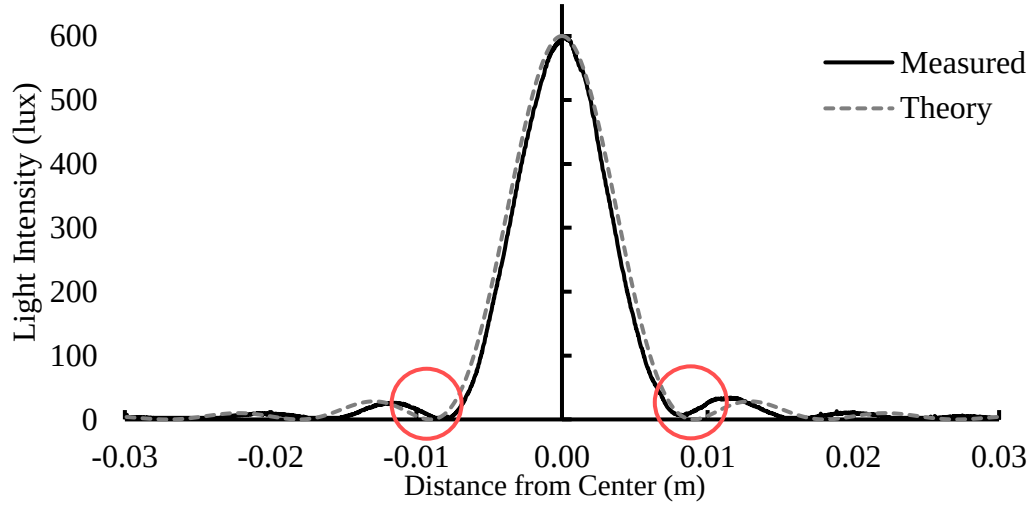

Figure 15: Measured intensity profile produced by a 100μm slit, shifted such that the distance from the center to the first minima on the left is the same as to the right.

Inspection shows that the asymmetry between the left and the right is reduced, but it is still present. This is evident from comparing the theoretical and the measured profiles at the regions highlighted by the red circles, as the left side matches the theory better than the right side. Fig. 16 below shows the comparison

between the location of the minima on either side. Even though the first minima are now symmetrical, the second and third minima on the left were 0.9% and 5.4% farther away from the center than those on the right, respectively. This suggests that the measured profile is still asymmetrical.

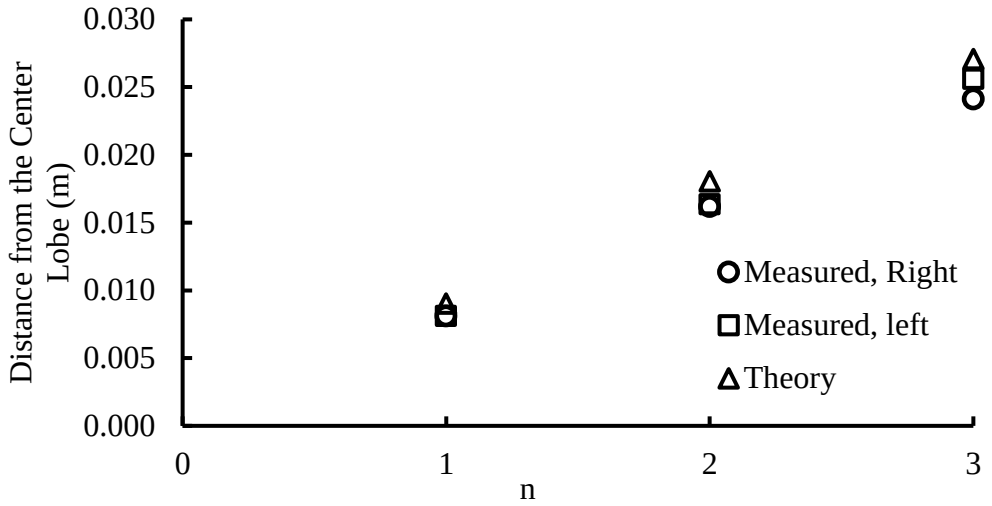

Figure 16: Comparison of the theoretical and the measured location of the intensity minima after the measured location has been further shifted.

Nonetheless, horizontally translating the measured intensity profiles such that the distance from the center lobe to the first intensity minima is the same on either side seems to reduce the asymmetry. Therefore, before we performed any further calculations, the measured profiles for all slit widths were shifted accordingly.

We wished to numerically assess whether the measured and the theoretical intensity profiles matched. Therefore, we decided to calculate the mean squared error (MSE) between the measured and the theoretical intensity profiles. The following is the equation for calculating MSE:

$$MSE = \frac{1}{n}\sum_{i=1}^{n}\left(I_i - \hat{I}_i\right)^2$$

where I_i represents the measured intensity and $\hat{I}_i$ represents the theoretical intensity. Table 2 below shows the MSE of each slit width.

Table 2: MSE between the theoretical and the measured profiles.

Slit width (μm)	**100**	**120**	**140**	**180**	**200**	**220**
MSE (lux^2)	40	18	23	99	67	26
MSE_{left} (lux^2)	62	32	54	57	120	50
MSE_{right} (lux^2)	22	8.3	5.3	150	31	9.2

We see that the MSE values are somewhat reasonable. Depending on the slit width, their MSE values are in the range of 15 to 100 lux^2. Considering they are squared values, they are reasonably small relative to the maximum intensity of the pattern, which is 600 lux.

We measured the ambient light intensity in the room to be 2.3 lux ± 0.1 lux. We could not vertically shift the intensity patterns such that the ambient intensity becomes 0 because the intensity at different intensity minima fluctuates randomly. Therefore, by default, the MSE value between the measured and the theoretical light intensity should be at least 5.3 lux^2 (or 2.3^2 lux^2) even if the theory and the measured intensities are a perfect match. This further suggests that the MSE values are reasonably small. Therefore, we concluded that the "sliding slit apparatus" is effective at measuring the single-slit diffraction pattern.

We also compared the MSE of the intensity profiles that are to the left of the center lobe with those to the right. We see that for all slit widths, aside from the 180μm slit, the MSE of the left-hand side is

significantly larger than that on the right-hand side. For the 180μm slit, the MSE of the right-hand side is significantly larger than that of the left-hand side. These corroborate with a previous observation: the measured intensity profiles are slightly asymmetrical, but we could not identify the cause of this asymmetry.

Although the apparatus is effective, it still has many sources of errors. The most significant source is the vibration from the linear actuator. Although the linear actuator maintained a constant horizontal velocity, its vertical velocity, caused by the vibration, was inconsistent. Visually, the vibration caused the entire apparatus to shake violently, such that it displaced the structure that it was mounted on by several centimeters after taking a few pre-trial measurements. We reinforced the structure to remain stationary during the actual experiment, but we suspect that it still affected the measurements. For example, the darker fringes beyond the third minima were visually well-defined on the screen, but they were undetectable by the light intensity sensor. In the case of the 220μm slit, there were 8 fringes on either side of the center lobe that were visible and within the range of motion of the linear actuator. However, beyond the fourth minima, the measurements were chaotically fluctuating. We believe this is likely caused by the vibrations from the linear actuator because we eliminated all other likely causes.

We eliminated the possibility that this chaotic fluctuation is caused by the light intensity sensor because for one trial for the 180μm slit, the sensor detected five clear minima on the left side and six on the right side. This shows it has the capability to detect these darker fringes. We also eliminated the effect of convolution as a cause of this fluctuation. We initially thought that since the effect of convolution would "blend" the intensity profile, such that with darker fringes, the minima "blended" in with the brighter part of its adjacent fringes. However, this is unlikely given for the second and third minima, the measured intensity minima spanned across multiple measurements, indicating these minima were small regions, not discrete points. Therefore, since the width of the fixed slit is only 70μm ± 5μm, it is unlikely that the minima were omitted because of the effect of convolution. Hence, we believe that this fluctuation must be caused by the vibrations from the actuator.

Conclusion

The theoretical intensity profile mostly matched with the intensity profile measured using the "sliding slit apparatus" for all slit widths that yielded analyzable measurements, without sensor saturation. The MSE values of the measurements were also reasonably small. However, there were some discrepancies between the measured and the theoretical intensity profiles. The measured profiles were slightly asymmetrical. We eliminated many possible causes of this asymmetry, but we could not explain it. We also noticed some chaotic fluctuations in the measurements of darker fringes. The vibration of the linear actuator is the most likely cause of this.

There are a few possible improvements for this apparatus. One of which would be replacing the current linear actuator with a pneumatic or compact-hydraulic actuator, because these actuators generate less vibration than the current configuration and their motion would be smoother and more reliable. This could reduce the fluctuations in measurements, especially for the darker fringes far away from the center lobe. This could also reduce the fluctuations and allow us to vertically shift the measured patterns such that the ambient light intensity becomes 0.

Another possible improvement is to substitute the neutral density filter with polarizers. We were unable to record analyzable measurements for the 160μm and the 240μm slits because we could not prevent the light intensity sensor from saturating. However, if we place two polarizers in front of the laser, and vary the angles between them, we could control the light transmittance ratio from fully transmitted to completely polarized. This means we could control the intensity more precisely, which would reduce sensor saturation. This also means that we could experimentally ensure that the maximum measured intensity is consistent between all slit widths.

In addition, even though the effect of convolution did not make a significant impact on the measured intensity profiles, we could factor its effect into the theory by finding the relationship between the theoretical diffraction pattern with the width of the sliding slit.

In conclusion, although there are a few flaws in the current apparatus, the "sliding slit apparatus" is effective at measuring the intensity profile of a single-slit diffraction pattern.

References

[1] Ling, S. J., Sanny, J., & Moebs, B. (2016). 4.1: Single-Slit Diffraction. In University physics volume 3 (pp. 142–146). essay, Rice University. Retrieved from https://openstax.org/books/university-physics-volume-3/pages/4-1-single-slit-diffraction

[2] Ghai, D. P., Senthilkumaran, P., & Sirohi, R. S. (2009). Single-slit diffraction of an optical beam with phase singularity. Optics and Lasers in Engineering, 47(1), 123–126. https://doi.org/10.1016/j.optlaseng.2008.07.019

[3] Williamson, J., Vokes, M., McDaid, C., & Mears, M. (2021). Razors and lasers: An undergraduate experiment to determine thermal expansion coefficients using single slit diffraction measurements. Physics Education, 57(1), 015002. https://doi.org/10.1088/1361-6552/ac27f7

[4] Mayes, T. W., & Melton, B. F. (1994). Fraunhofer diffraction of visible light by a narrow slit. American Journal of Physics, 62(5), 397–403. https://doi.org/10.1119/1.17539

[5] Konijnenberg, S., Adam, A. J. L., & Urbach, H. P. (2022, September 16). 6.7: Fraunhofer diffraction revisited. Physics LibreTexts. Retrieved October 15, 2022, from https://phys.libretexts.org/Bookshelves/Optics/BSc_Optics_(Konijnenberg_Adam_and_Urbach)/06%3A_Scalar_diffraction_optics/6.08%3A_Fraunhofer_Diffraction_Revisited

[6] Ling, S. J., Sanny, J., & Moebs, B. (2016). 4.2: Intensity in Single-Slit Diffraction. In University physics volume 3 (pp. 142–146). essay, Rice University. Retrieved from https://openstax.org/books/university-physics-volume-3/pages/4-2-intensity-in-single-slit-diffraction

[7] Ellingson, S. W. (2022, September 12). 1.5: Phasors. Engineering LibreTexts. Retrieved November 24, 2022, from https://eng.libretexts.org/Bookshelves/Electrical_Engineering/Electro-Optics/Book%3A_Electromagnetics_I_(Ellingson)/01%3A_Preliminary_Concepts/1.05%3A_Phasors

[8] Logger Pro 3. Vernier Science Education. (2022). Retrieved November 28, 2022, from https://www.vernier.com/product/logger-pro-3/

[9] Allen, R. (2022, October 11). Convolution. from Wolfram MathWorld. Retrieved October 15, 2022, from https://mathworld.wolfram.com/Convolution.html